Modulation of Triple-Helical Stability and Subsequent Melanoma Cellular Responses by Single-Site Substitution of Fluoroproline Derivatives†

Navdeep B. Malkar, Janelle L. Lauer-Fields, Jeffrey A. Borgia, and Gregg B. Fields*

Department of Chemistry and Biochemistry, Florida Atlantic University, 777 Glades Road, Boca Raton, Florida 33431-0991

Received November 19, 2001; Revised Manuscript Received February 19, 2002

ABSTRACT: Collagen is a multifunctional protein, serving as a structural scaffold and a modulator of cellular responses. Prior work has identified distinct regions from several collagen types that promote cell adhesion, spreading, migration, and signal transduction. One of these regions, α1(IV)1263−1277 from type IV collagen, mediates these responses via melanoma cell CD44−chondrotin sulfate proteoglycan receptors. In the study presented here, we have used a triple-helical model of α1(IV)1263−1277 to evaluate (a) conformational stability and (b) cellular responses based on single-site incorporation of *trans*-4-fluoro-L-proline (*trans*-Flp) or *cis*-4-fluoro-L-proline (*cis*-Flp) for *trans*-4-hydroxy-L-proline (*trans*-Hyp). The structural effects of *cis*-Flp and *trans*-Flp substitution were studied by circular dichroism and NMR spectroscopies. The peptide containing a single *trans*-Flp instead of *trans*-Hyp was slightly more thermally stable than the parent peptide ($T_m = 37$ vs 34 °C), while the peptide containing *cis*-Flp was considerably less stable than the parent peptide ($T_m = 30$ °C). Melanoma cell adhesion and spreading were examined under conditions where the *trans*-Hyp-, *trans*-Flp-, and *cis*-Flp-containing ligands were ∼15, <10, and ∼65% denatured, respectively. Adhesion to each of the three ligands was remarkably sensitive to the respective ligand conformation, with EC_{50} values of ∼2.5, ∼0.35, and >5.0 μM for the *trans*-Hyp-, *trans*-Flp-, and *cis*-Flp-containing ligands, respectively. Melanoma cell spreading was quantitated over a ligand concentration range of 0.01−50 μM and, in a fashion similar to adhesion, was more extensive on the *trans*-Flp ligand than on the *trans*-Hyp ligand. Very low levels of spreading were observed with the *cis*-Flp-containing ligand at all concentrations tested. Melanoma cell adhesion to and spreading on the three ligands suggested the dramatic biological consequence of even subtle changes in relative triple-helical content. Such subtle changes may model those occurring in the basement membrane during the tumor cell invasion process, and thus provide mechanistic insight into this stage of metastasis.

Tumor cell invasion, a key step in the metastatic process, involves a complex series of correlated macromolecular interactions. These interactions result in tumor cell surface receptor recognition of extracellular matrix components, induction of "outside-in" signal transduction, dissolution of the extracellular matrix, and promotion of tumor cell motility. To better understand tumor cell behavior, numerous model systems have been designed, each approximating one specific step or series of steps in the invasion process. In general, such systems may be significant in two regards; they aid in a molecular understanding of biochemical mechanisms, and they guide the design of inhibitory molecules. There is a long history of model system development for better understanding the physiological roles of collagen. Collagen is the most abundant protein in vertebrates, and functions as both a structural scaffold and modulator of cellular activities. Tumor cell invasion involves interaction with, and movement through, collagen, most often type I and/or basement membrane (type IV) collagen.

The most prominent feature of collagen is its unique triple-helical structure, resulting from the intertwining of three poly-Pro II-like peptide strands in a helical structure that twists in a right-handed manner. The individual strands of the triple helix are composed of Gly-Xxx-Yyy repeating sequences. To better define the forces that contribute to triple-helical stability, peptide models of collagen have been constructed using the Gly-Xxx-Yyy repeating sequence (*1*−*6*). Peptide models have also been developed to correlate triple-helical structure and collagen-mediated biological activities, such as cell adhesion and activation (*7*−*15*). In cases of cell adhesion and activation, model studies have examined the overall role of the triple helix by incorporating analogous collagen-derived sequences into clustered triple-helical, monomeric triple-helical, and non-triple-helical peptides (*7*−*9*, *11*−*13*, *16*, *17*). The effects of subtle variations in triple-helical structure on cellular systems have not been addressed. Such variations may be relevant for the physiological modeling of the invasion process, specifically after the basement membrane is compromised. To analyze triple-helical variations, one may utilize a biologically active "host" sequence in which single-amino acid substitutions can either enhance or diminish triple-helical stability. Cellular activities associated with the invasion process can then be quantitated as a function of triple-helical content.

† This research was supported by grants from the National Institutes of Health (CA 77402 and AR 01929 to G.B.F.).

* To whom correspondence should be addressed: Department of Chemistry and Biochemistry, Florida Atlantic University, 777 Glades Rd., Boca Raton, FL 33431-0991. Telephone: (561) 297-2093. Fax: (561) 297-2759. E-mail: fieldsg@fau.edu.

10.1021/bi012071w CCC: $22.00
Published on Web 04/23/2002

The effects of single-site substitution of naturally occurring amino acids on triple-helix nucleation and stability have been examined previously using a host−guest approach, where either Pro in the Xxx or 4-hydroxy-L-proline (Hyp)[1] in the Yyy position of a Gly-Pro-Hyp triplet is replaced with the "guest" residue (*18*, *19*). Of the 20 natural amino acids that were studied, none provided either enhanced stability or more rapid nucleation than the Gly-Pro-Hyp sequence. The non-native amino acid *trans*-4-amino-L-proline is more stabilizing than Hyp for Phe-(Pro-Yyy-Gly)$_6$ triple helices (*20*). Interestingly, β-D-galactose glycosylation of Thr in the Yyy position of the (Gly-Pro-Yyy)$_{10}$ peptide greatly enhances triple-helical stability compared to that of Thr (*21*, *22*). The non-native amino acid *trans*-4-fluoro-L-proline (*trans*-Flp) has been shown to induce hyperstability in the triple helix of the (Pro-Flp-Gly)$_{10}$ peptide compared to the (Pro-Hyp-Gly)$_{10}$ peptide (*4*, *5*). Alternatively, *cis*-Flp destabilizes the triple helix of the (Pro-Flp-Gly)$_7$ peptide compared to the (Pro-Hyp-Gly)$_7$ peptide (*23*). In general, the use of fluorine-based amino acids for construction of model proteins has received a great deal of recent attention. Fluorinated residues have been utilized to enhance hydrophobic stabilization of coiled coil proteins (*24*−*26*). Since fluorine-containing molecules have a wide range of chemical shifts (~1000 ppm compared to 15 ppm for protons), they are more sensitive to their environment than protons, and fluorinated probes can be valuable for ^{19}F NMR conformational analyses of peptides and proteins (*27*−*29*). Also, a combination of electron microscopy and electron energy-loss spectroscopy has been used to visualize specific platelet intracellular localization of the fluorine tracer of 4,6-difluoroserotonin (*30*). Thus, fluorinated peptides are potentially useful for localizing cellular binding sites, which could prove valuable for studies of triple-helical cellular ligands. Flp residues, in either the *cis* or *trans* form, could be used to modulate triple-helical structure and function. However, neither the structural nor biological consequences of single-Flp substitutions are known.

Human melanoma cells have been shown to bind to distinct triple-helical regions within type IV (basement membrane) collagen (*7*, *8*, *10*, *12*, *31*). Interaction with and invasion of basement membrane collagen is believed to be a critical step in the metastatic process. One region from type IV collagen, the α1(IV)1263−1277 sequence [Gly-Val-Lys-Gly-Asp-Lys-Gly-Asn-Pro-Gly-Trp-Pro-Gly-Ala-Pro (designated [IV-H1])], promotes melanoma cell adhesion, spreading, and signaling (*7*, *10*, *32*−*34*). Affinity chromatography studies with [IV-H1] resulted in the isolation of melanoma cell CD44 receptors, in the chondrotin sulfate proteoglycan form (*31*, *35*, *36*). Several triple-helical constructs incorporating the [IV-H1] sequence have been described (*7*, *12*, *34*). One type of construct, a "peptide−amphiphile" construct of general structure H_3C-$(CH_2)_{n-2}$-C(O)-(Gly-Pro-Hyp)$_4$-[IV-H1]-(Gly-Pro-Hyp)$_4$-NH_2, has undergone extensive biophysical characterization by CD and one- and two-dimensional NMR spectroscopies (*37*−*39*). When incorporated into the peptide−amphiphile construct, the [IV-H1] region forms a continuous triple helix (*38*, *39*). Loss of triple-helical structure dramatically reduces the level of melanoma cell adhesion, spreading, and signaling modulated by this ligand (*7*, *34*). Thus, a H_3C-$(CH_2)_{n-2}$-C(O)-(Gly-Pro-Hyp)$_4$-[IV-H1]-(Gly-Pro-Hyp)$_4$-NH_2 "host" could be used to evaluate the structural and biological consequences of single-site substitutions. For studying melanoma cell activities, it would be desirable to compare substitutions that enhance triple-helix stability versus substitutions that diminish stability.

This study has sought to measure the effects of a single-amino acid substitution on the triple helix. We wished to understand both the structural and biological consequences of replacing a single Hyp residue in the Yyy position with Flp. For this purpose, the host peptide was (Gly-Pro-Hyp)$_3$-Gly-Pro-Yyy-[IV-H1]-(Gly-Pro-Hyp)$_4$-NH_2. The residue in the Yyy[12] position was *trans*-Hyp, *cis*-Flp, or *trans*-Flp. Since both *cis*-Flp and *trans*-Flp are required for this study, we first examined more efficient methods for the preparation of 9-fluorenylmethoxycarbonyl (Fmoc) and *tert*-butyloxycarbonyl (Boc) Flp derivatives. The desired peptides and peptide−amphiphile constructs were then assembled, and biophysical comparisons were performed using CD and NMR spectroscopies to determine the conformational effects of single-site Flp incorporation. Last, melanoma cell adhesion and spreading on the respective peptide−amphiphile ligands were quantitated to (a) determine the biological consequences of Hyp replacement with Flp and (b) correlate ligand conformation with cellular activities.

MATERIALS AND METHODS

General. All reactions were carried out under an inert atmosphere and anhydrous conditions with dry solvents unless otherwise stated. Thin-layer chromatography (TLC) was performed on Polygram Sil G/UV254 (Macherey-Nagel) with detection by UV light. Organic solutions were dried over anhydrous Na_2SO_4 before being concentrated. *cis*-Hyp, morpholinosulfur trifluoride, and palmitic acid [CH_3-$(CH_2)_{14}$-CO_2H, designated C_{16}] were purchased from Aldrich. Electrospray mass spectra (ESMS) were recorded in the positive mode on a Finnigan MAT LCQ Deca mass spectrometer, with 0.1% acetic acid in water as the liquid phase. All standard peptide synthesis chemicals were peptide synthesis grade or better and purchased from FisherBiotech (La Jolla, CA). 1-Hydroxybenzotriazole (HOBt) and *N*-[(1*H*-benzotriazol-1-yl)(dimethylamino)methylene]-*N*-methylmethanaminium hexafluorophosphate *N*-oxide (HBTU) were purchased from Quantum Biotechnologies (Montreal, PQ), and *N*,*N*-diisopropylethylamine (DIEA) was from Fisher Scientific. *trans*-Hyp-OBzl, Fmoc-4-[(2′,4′-dimethoxyphenyl)aminomethyl]phenoxy resin (substitution level, 0.55 mmol/g), Fmoc-*N*-hydroxysuccinimide ester (Fmoc-ONSu), and Fmoc-labeled amino acid derivatives were purchased from Novabiochem (La Jolla, CA). Amino acids are of the L-configuration (except for Gly). Ammonium formate, 10% Pd/C, and di-*tert*-butyl dicarbonate were from Acros Organics (Fair Lawn, NJ).

[1] Abbreviations: Boc, *tert*-butyloxycarbonyl; Bzl, benzyl; CD, circular dichroism; CTH, catalytic transfer hydrogenation; DAST, diethylaminosulfur trifluoride; DIEA, *N*,*N*-diisopropylethylamine; DMF, *N*,*N*-dimethylformamide; ESMS, electrospray mass spectrometry; Flp, 4-fluoro-L-proline; Fmoc, 9-fluorenylmethoxycarbonyl; Fmoc-ONSu, Fmoc *N*-hydroxysuccinimide ester; HBTU, 2-(1*H*-benzotriazol-1-yl)-1,1,3,3-tetramethyluronium hexafluorophosphate; HOBt, 1-hydroxybenzotriazole; Hyp, 4-hydroxy-L-proline; [IV-H1], α1(IV)1263−1277 collagen sequence Gly-Val-Lys-Gly-Asp-Lys-Gly-Asn-Pro-Gly-Trp-Pro-Gly-Ala-Pro; MALDI-MS, matrix-assisted laser desorption/ionization mass spectrometry; NMR, nuclear magnetic resonance; PTH, phenylthiohydantoin; RP-HPLC, reversed-phase high-performance liquid chromatography; TFA, trifluoroacetic acid; TLC, thin-layer chromatography.

Preparation of cis-4(S)-Hydroxy-L-proline Benzyl Ester (cis-Hyp-OBzl) ***2b***. *cis*-4(*S*)-Hydroxy-L-proline (**1b**, 0.5 g, 3.81 mmol) was dissolved in 10 mL of 10% $NaHCO_3$ and cooled to 0−4 °C. Benzyl bromide (0.652 g, 3.81 mmol) dissolved in cold (4 °C) *N*,*N*-dimethylformamide (DMF) (10 mL) was then added slowly. The mixture was stirred at 4 °C for 30 min and then overnight at room temperature. DMF was evaporated in vacuo at room temperature, and water (15 mL) was added to the resulting residue. The aqueous phase was extracted with ethyl acetate (2 × 20 mL). The ethyl acetate layer was dried over anhydrous sodium sulfate and evaporated in vacuo at room temperature to give *cis*-Hyp-OBzl (**2b**, 0.75 g, 3.38 mmol, 88%).

Preparation of Fmoc-cis-4(S)-Hydroxy-L-proline Benzyl Ester (Fmoc-cis-Hyp-OBzl) ***3b***. *cis*-Hyp-OBzl (**2b**, 0.644 g, 2.50 mmol) was dissolved in 30 mL of 10% Na_2CO_3 and cooled to 4 °C. Fmoc-ONSu (1.89 g, 5.6 mmol) dissolved in cold (4 °C) dimethoxyethane (30 mL) was added slowly. The mixture was stirred at 4 °C for 4 h and then overnight at room temperature. The resulting suspension was filtered and acidified to pH ∼3 with HCl. Dimethoxyethane was evaporated in vacuo at room temperature, and the reaction mixture was extracted with ethyl acetate (2 × 40 mL). The ethyl acetate layer was dried over anhydrous sodium sulfate and evaporated in vacuo at room temperature to give Fmoc-*cis*-Hyp-OBzl (**3b**, 1.03 g, 2.32 mmol, 93%).

Preparation of Fmoc-trans-4(R)-Fluoro-L-proline Benzyl Ester (Fmoc-trans-Flp-OBzl) ***4b***. The hydroxyl group in Fmoc-*cis*-Hyp-OBzl was converted into a fluoro group using the morpholino analogue of DAST (*40*). Morpholinosulfur trifluoride (0.564 g, 3.22 mmol) was added dropwise over 10 min with constant stirring to a solution (5 mL) of CH_2Cl_2 containing Fmoc-Hyp-OBzl (**3b**) at −80 °C under nitrogen. The reaction mixture was allowed to warm to room temperature, further stirred for 48 h, and concentrated under reduced pressure, and the reaction was quenched with water (2 mL). The diluted reaction mixture was then evaporated in vacuo at room temperature and subjected to flash chromatography [1:4 (v/v) ethyl acetate/hexane mixture] to give Fmoc-*trans*-Flp-OBzl (**4b**, 0.849 g, 1.90 mmol, 83%).

Preparation of Fmoc-trans-4(R)-Fluoro-L-proline (Fmoc-trans-Flp) ***5b***. Hydrogenation of Fmoc-*trans*-Flp-OBzl to Fmoc-*trans*-Flp was achieved using ammonium formate as the hydrogen donor and Pd/C as the heterogeneous catalyst. Fmoc-*trans*-Flp-Obzl (**4b**) was dissolved in methanol (5 mL). Ten percent Pd/C (0.100 g) was added, followed by the addition of ammonium formate (0.471 g, 7.46 mmol) at room temperature. The reaction mixture was stirred for 2 h at room temperature. After completion of hydrogenolysis (monitored using TLC), the mixture was filtered through Celite and the catalyst was washed with methanol (2 × 10 mL). The combined filtrates were evaporated in vacuo at room temperature to minimal volume and extracted with ethyl acetate (2 × 25 mL). The ethyl acetate extract was washed with a saturated sodium chloride solution (2 × 10 mL) and dried with sodium sulfate. The ethyl acetate was evaporated in vacuo at room temperature to give Fmoc-*trans*-Flp (**5b**, 0.64 g, 1.81 mmol, 95%). The overall yield was 65%. ^{1}H NMR analysis for **5b** (300 MHz, CD_3OD): δ 7.31−7.78 (m, 8H, Fmoc-ArH), 4.56 (m, 1H, =CH-F), 4.48 (m, 1H, Fmoc-CH), 4.33−4.43 (m, 2H, Fmoc-CH_2), 4.28 (dt, 1H, =CH-COOH), 3.55−3.78 (dd, 2H, -CH_2), 2.30−2.48, 2.17 (m, 2H, -CH_2-). ESMS gave $[M + H]^+ = 356$ Da (theoretical, 355.12 Da). For comparison, ESMS of commercially available Fmoc-Hyp gave $[M + H]^+ = 351.8$ Da (theoretical, 353.13 Da).

Preparation of Fmoc-cis-4(S)-Fluoro-L-proline (Fmoc-cis-Flp) ***5a***. Fmoc-*cis*-Flp was prepared from *trans*-Hyp-OBzl (**2a**) in a fashion similar to the preparation of Fmoc-*trans*-Flp from *cis*-Hyp-OBzl. ^{1}H NMR analysis for **5b** (300 MHz, CD_3OD): δ 7.31−7.78 (m, 8H, Fmoc-ArH), 4.56 (m, 1H, =CH-F), 4.47 (m, 1H, Fmoc-CH), 4.31−4.43 (m, 2H, Fmoc-CH_2), 4.27 (dt, 1H, =CH-COOH), 3.56−3.75 (dd, 2H, -CH_2), 2.29−2.45, 2.17 (m, 2H, -CH_2-). ESMS gave $[M + H]^+ = 356$ Da (theoretical, 355.12 Da).

Preparation of Boc-cis-4(S)-Fluoro-L-proline (Boc-cis-Flp) ***5c***. Hyp-OBzl (0.644 g, 2.50 mmol) was dissolved in 30 mL of 10% Na_2CO_3 and cooled to 4 °C. Procedures were then identical to those for Fmoc-*cis*-Flp preparation, except that di-*tert*-butyl dicarbonate (0.6 g, 2.75 mmol) in 7 mL of dimethoxyethane was used instead of Fmoc-ONSu. The overall product yield of **5c** was 71%. ^{1}H NMR analysis for **5c** (300 MHz, CD_3OD): δ 8.56 (b, 1H, -COOH), 4.22 (m, 1H, =CH-COOH), 3.42 (dm, 1H, =CH-F), 3.51 (bm, 2H, -CH_2-), 1.98 (m, 2H, -CH_2-), 1.40 (s, 9H, Boc-CH_3). ESMS gave $[M + H]^+ = 232.8$ Da (theoretical, 233.12 Da).

Peptide Synthesis, Purification, and Characterization. Peptide resin assembly was performed by Fmoc solid-phase methodology on a Perkin-Elmer/ABD 433A peptide synthesizer by methods previously described in our laboratory (*37*, *38*). Peptides were synthesized as C-terminal amides to prevent diketopiperazine formation (*41*). Peptide resins were characterized by Edman degradation sequence analysis as described previously for "embedded" (noncovalent) sequencing (*42*) on an Applied Biosystems 477A protein sequencer/120A analyzer. Peptide resins were then either (a) cleaved or (b) acylated with the C_{16} alkyl tail (*38*) and then cleaved. Cleavage and side chain deprotection of the peptide resin proceeded for 2 h using an ethanedithiol/thioanisole/phenol/water/TFA mixture (2.5:5:5:5:82.5) as described previously (*43*). The cleavage solution was extracted with methyl *tert*-butyl ether prior to purification.

RP-HPLC purification was performed on a Rainin Auto-Prep System. The peptide was purified with a Vydac 218TP152022 C_{18} column (15−20 μm particle size, 300 Å pore size, 250 mm × 25 mm) at a flow rate of 5.0 mL/min. The elution gradient was 0 to 85% B in 85 min, where A was 0.1% trifluoroacetic acid (TFA) in water and B was 0.1% TFA in acetonitrile. Detection was at 229 nm. Analytical RP-HPLC was performed on a Hewlett-Packard 1100 liquid chromatograph equipped with an ODS Hypersil C_{18} RP column (5 μm particle size, 120 Å pore size, 100 mm × 2.1 mm). Eluants were the same as for peptide purification. The elution gradient was 0 to 100% B in 30 min with a flow rate of 0.3 mL/min. Diode array detection was at 220, 254, and 280 nm.

Matrix-assisted laser desorption/ionization mass spectrometry (MALDI-MS) was performed on a Hewlett-Packard G2025A LD-TOF mass spectrometer using either a sinapinic acid or 2,5-dihydroxybenzoic acid/2-hydroxy-5-methoxybenzoic acid (9:1, v/v) matrix (*44*). Peptide mass values were as follows: $(Gly\text{-}Pro\text{-}Hyp)_4$-[IV-H1]-$(Gly\text{-}Pro\text{-}Hyp)_4$-$NH_2$, $[M + H]^+ = 3573.3$ Da (theoretical, 3574.9 Da); $(Gly\text{-}Pro\text{-}Hyp)_3$-Gly-Pro-[*cis*-Flp]-[IV-H1]-$(Gly\text{-}Pro\text{-}Hyp)_4$-$NH_2$, [M +

$H]^+ = 3577.4$ Da (theoretical, 3576.9 Da); (Gly-Pro-Hyp)$_3$-Gly-Pro-[*trans*-Flp]-[IV-H1]-(Gly-Pro-Hyp)$_4$-NH_2, $[M + H]^+ = 3577.2$ Da (theoretical, 3576.9 Da); C_{16}-(Gly-Pro-Hyp)$_4$-[IV-H1]-(Gly-Pro-Hyp)$_4$-NH_2, $[M + H]^+ = 3808.4$ Da (theoretical, 3813.3 Da); C_{16}-(Gly-Pro-Hyp)$_3$-Gly-Pro-[*cis*-Flp]-[IV-H1]-(Gly-Pro-Hyp)$_4$-NH_2, $[M + Na]^+ = 3834.8$ Da (theoretical, 3837.3 Da); and C_{16}-(Gly-Pro-Hyp)$_3$-Gly-Pro-[*trans*-Flp]-[IV-H1]-(Gly-Pro-Hyp)$_4$-NH_2, $[M + H]^+ = 3816.2$ Da (theoretical, 3815.3 Da).

CD Spectroscopy. CD spectra were recorded over the wavelength range of 190−250 nm on a JASCO J-600 instrument using a 10 mm path length quartz cell. The peptide concentration (3.41 μM in H_2O) was kept constant for all the experiments. Thermal transition curves were obtained by recording the molar ellipticity ([θ]) at 225 nm, while the temperature was continuously increased in the range of 5−80 °C at a rate of 12 °C/h. The temperature was controlled using a JASCO PTC-348WI temperature control unit. For samples exhibiting sigmoidal melting curves, the reflection point in the transition region (first derivative) is defined as the melting temperature (T_m). Alternatively, T_m was evaluated from the midpoint of the transition.

NMR Spectroscopy. ^{1}H and ^{13}C NMR spectra for amino acid derivatives were acquired on a 300 MHz Varian Inova spectrometer at 300 K for solutions in $CDCl_3$, CD_3OD, or D_2O (Aldrich). ^{1}H chemical shifts were expressed relative to tetramethylsilane as an internal standard. Peptide ^{1}H and ^{19}F NMR spectra were acquired on a 500 MHz Varian Inova spectrometer at room temperature. Freeze-dried samples were dissolved in a D_2O/H_2O mixture (1:9) at concentrations of 0.5−3 μM, depending upon the solubility of the peptides and peptide−amphiphile constructs. ^{1}H and ^{19}F chemical shifts were expressed relative to sodium 3-(trimethylsilyl)-tetradeuteriopriopionate and hexafluorobenzene, respectively.

Cells. SK-Mel2 human melanoma cells were propagated as described previously (*12*). Briefly, melanoma cells were cultured in EMEM supplemented with 10% fetal bovine serum, 1 mM sodium pyruvate, 0.1 mg/mL gentamicin, 50 units/mL penicillin, and 0.05 mg/mL streptomycin. Cells were passaged eight times and then replaced from frozen stocks of early passage cells to minimize phenotypic drift. All cells were maintained at 37 °C in a humidified incubator containing 5% CO_2. All media reagents were purchased from Fisher Scientific (Atlanta, GA).

Cell Adhesion Assays. Melanoma cell adhesion to substrate-coated Immulon 96-well plates (Dynatech) was performed as described previously (*12*). Peptide−amphiphile constructs dissolved in PBS were diluted in 70% ethanol, added to the 96-well plate, and allowed to adsorb overnight at room temperature with mixing. Nonspecific binding sites were blocked with 2 mg/mL ovalbumin in PBS for 2 h at 37 °C. Cells were released with 5 mM EDTA in PBS, washed twice with adhesion medium (20 mM HEPES, 1 mM sodium pyruvate, and 2 mg/mL ovalbumin in EMEM), and labeled with 5- or 6-carboxyfluorescein diacetate. Unincorporated fluorophore was removed with repeated washings of adhesion medium. Cells were then resuspended in adhesion medium and added to the plate. The plate was incubated for 60 min at 37 °C. Nonadherent cells were removed by washing three times with adhesion medium. Adherent cells were lysed with 0.2% SDS and quantitated with a SpectraMAX Gemini, 96-well plate spectraflurometer (Molecular Devices).

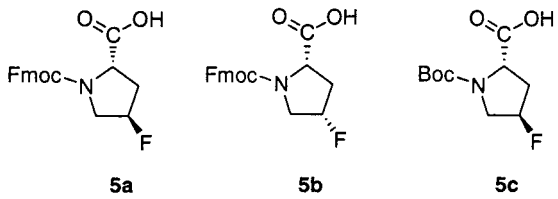

5a **5b** **5c**

FIGURE 1: Structures of Fmoc-*cis*-4(*S*)-fluoroproline (**5a**), Fmoc-*trans*-4(*R*)-fluoroproline (**5b**), and Boc-*cis*-4(*S*)-fluoroproline (**5c**).

Cell Spreading Assays. These assays are performed exactly as the adhesion assays with the exception of the last step, cell lysis. After unbound cells are washed, the remaining cells are fixed with 2.5% glutaraldehyde diluted in formalin, and stained with R-250 Coomassie Blue. Digital photos of each well are taken, and the area of the cells is quantitated with the assistance of Quantity One software (Bio-Rad).

RESULTS

Synthesis of Flp Derivatives. To efficiently incorporate Flp into peptides, convenient synthetic routes for the production of derivatized Flp residues (Figure 1), such as Fmoc-*cis*-Flp (**5a**), Fmoc-*trans*-Flp (**5b**), and Boc-*cis*-Flp (**5c**), would be most desirable. Initial methods reported for the synthesis of fluoro- and difluoroprolines started from *N*-acetyl (*45*−*47*), benzoyl (*48*), or benzyloxycarbonyl (*49*) Hyp methyl esters or Hyp-derived diketopiperazines (*50*) and oxazolidinones (*51*). Avent et al. reported the direct fluorination of Boc-4-hydroxypyroglutamic acid in moderate yield (40%) (*52*). Taking advantage of the direct fluorination route using diethylaminosulfur trifluoride (DAST) (*40*), Demange et al. converted Boc-*trans*-Hyp-OCH_3 to Boc-*cis*-Flp-OCH_3 in 81% yield (*53*). Saponification of the methyl ester was achieved in 92% yield. To prepare Fmoc-*cis*-Flp, the Boc group was removed with TFA and the Fmoc group added with Fmoc-ONSu (*53*). Fmoc-*cis*-Flp was obtained in 65% yield. Tran et al. prepared Fmoc-*cis*-Flp and Fmoc-*trans*-Flp directly from the appropriate Fmoc-Hyp-OCH_3 derivatives using DAST (*54*). The methyl ester was removed by treatment with refluxing 6 N HCl (*54*).

We envisioned slightly more convenient synthetic routes for the preparation of Fmoc-*cis*-Flp and Fmoc-*trans*-Flp, and a more practical one for Boc-*cis*-Flp, from readily available *trans*-Hyp-OBzl or *cis*-Hyp. For the preparation of Fmoc-*cis*-Flp, we proposed a three-step synthesis comprised of Fmoc addition to *trans*-Hyp-OBzl, conversion of the hydroxyl group to a fluoro group, and debenzylation (Scheme 1). The first step was achieved by a straightforward reaction of Fmoc-ONSu with Hyp-OBzl. The second step, direct fluorination of an Fmoc-labeled amino acid, had been described previously (*54*). The Fmoc group appeared to be completely stable to the conditions of the morpholinosulfur trifluoride reaction, and thus, conversion of the hydroxyl to a fluoro group was not complicated. The third step, debenzylation, was the most problematic. The Fmoc group is stable to allyl transfer reactions using $(Ph_3P)PdCl_2$ or $(Ph_3P)_4Pd$ (*55*), but is not completely stable to standard Pd/C hydrogenation reactions (*56*, *57*). Of the conditions that were tested, hydrogenation of Fmoc-aniline in an acetic acid/methanol mixture (1:4) resulted in the slowest removal of the Fmoc group (*57*). We believed that the relatively mild conditions of ammonium formate catalytic transfer hydro-

Scheme 1: Synthesis of Fmoc-4-Fluoroproline (Flp) Derivatives

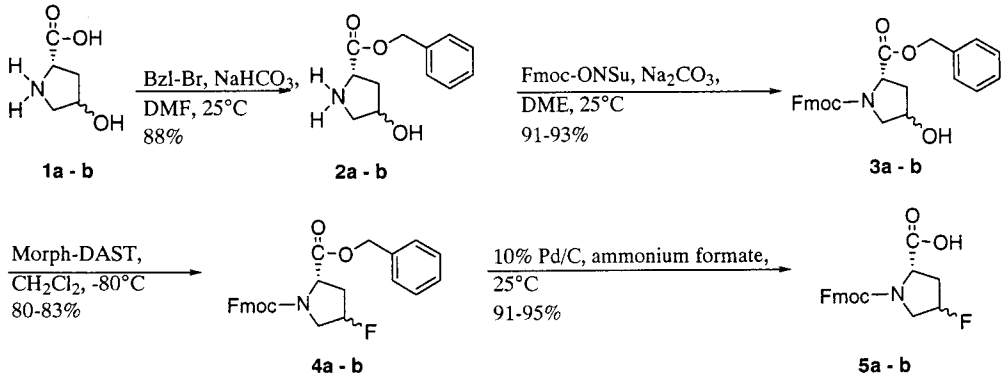

Table 1: Elution of PTH-Hyp and PTH-Flp Derivatives

PTH derivative	retention time, early peak (min)	retention time, late peak (min)	molar ratio (early peak/late peak)
cis-Hyp	7.88	9.08	1.25
cis-Flp	7.73	8.92	1.18
trans-Hyp	7.77	8.97	0.40
trans-Flp	7.81	9.00	0.40

genation (CTH) (*58*, *59*) in methanol may result in minimal loss of the Fmoc group. We found that removal of the benzyl ester using ammonium formate CTH for 2 h was highly efficient, and that the Fmoc group appeared to be relatively stable to these conditions. Fmoc-*cis*-Flp was obtained in 65% overall yield by this procedure (Scheme 1). Fmoc-*trans*-Flp was prepared in one additional step, where the starting material (*cis*-Hyp) first needed conversion to the benzyl ester (Scheme 1).

Synthesis of Boc-*cis*-Flp followed the same basic three-step approach used for Fmoc-*cis*-Flp. Boc-Hyp-OBzl was synthesized by treatment of Hyp-OBzl with di-*tert*-butyl dicarbonate. Conversion of Boc-Hyp-OBzl to Boc-Flp-OBzl was achieved by reaction with morpholinosulfur trifluoride. Ammonium formate CTH was then used to remove the benzyl group. Prior studies have shown that the Boc group is stable to both DAST and ammonium formate CTH reaction conditions (*53*, *58*, *59*). Boc-Flp was obtained in 71% overall yield. The procedure described here for Boc-Flp derivatives is very similar to one described by Demange et al. (*53*), except that we chose to work with the benzyl ester of Hyp rather than the methyl ester.

Construction of Flp-Containing Peptides. Fmoc-Flp derivatives **5a** and **5b** were used for the synthesis of the collagen model sequence (Gly-Pro-Hyp)$_3$-Gly-Pro-Flp-Gly-Val-Lys-Gly-Asp-Lys-Gly-Asn-Pro-Gly-Trp-Pro-Gly-Ala-Pro-(Gly-Pro-Hyp)$_4$-NH_2 [(Gly-Pro-Hyp)$_3$-Gly-Pro-Flp-[IV-H1]-(Gly-Pro-Hyp)$_4$-NH_2]. The analogous sequence containing *trans*-Hyp instead of the Flp residues has been synthesized previously and structurally characterized by CD and NMR spectroscopies (*37*−*39*). Synthesis of the peptides proceeded without difficulty, and Edman degradation sequence analysis of the peptide resins indicated a highly efficient assembly. Interestingly, each of the PTH-Flp residues eluted as two peaks in positions similar to the two peaks seen for PTH-Hyp (Table 1) (*42*, *60*). By comparison to *cis*-Hyp and *trans*-Hyp standards, it appears that the *cis* derivatives elute earlier and the *trans* derivatives elute later (Table 1). Interconversion between the *cis* and *trans* forms occurs during the derivatization of the amino acid to its PTH form. The peptides were subsequently purified by RP-HPLC, and characterized by MALDI-MS.

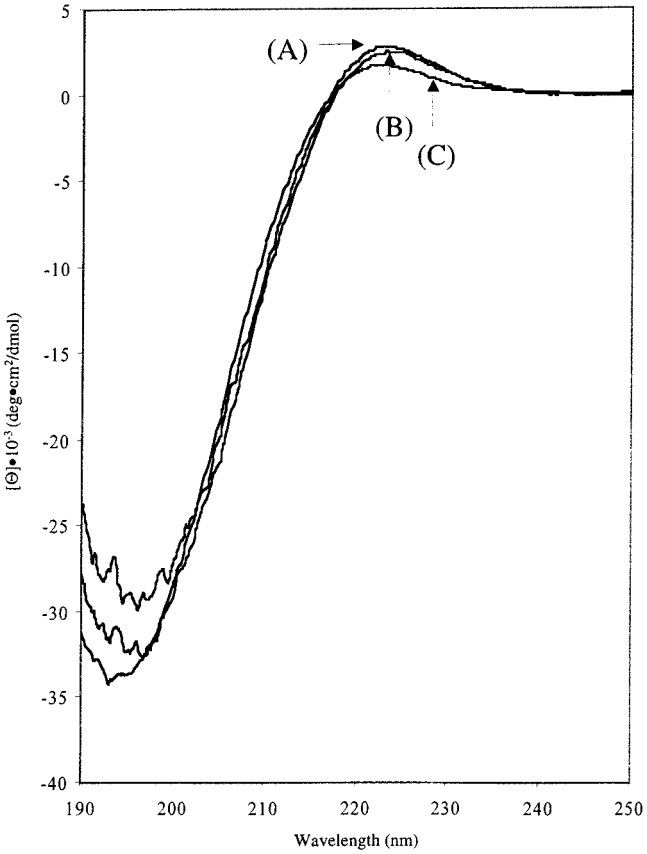

FIGURE 2: Circular dichroism spectra of (A) (Gly-Pro-Hyp)$_3$-Gly-Pro-[*trans*-Flp]-[IV-H1]-(Gly-Pro-Hyp)$_4$-NH_2, (B) (Gly-Pro-Hyp)$_4$-[IV-H1]-(Gly-Pro-Hyp)$_4$-NH_2, and (C) (Gly-Pro-Hyp)$_3$-Gly-Pro-[*cis*-Flp]-[IV-H1]-(Gly-Pro-Hyp)$_4$-NH_2 at 5 °C. Peptide concentrations were 3.41 μM in H_2O.

Biophysical Characterization. CD spectra were obtained for (Gly-Pro-Hyp)$_4$-[IV-H1]-(Gly-Pro-Hyp)$_4$-NH_2, (Gly-Pro-Hyp)$_3$-Gly-Pro-[*trans*-Flp]-[IV-H1]-(Gly-Pro-Hyp)$_4$-NH_2, and (Gly-Pro-Hyp)$_3$-Gly-Pro-[*cis*-Flp]-[IV-H1]-(Gly-Pro-Hyp)$_4$-NH_2 at 5 °C (Figure 2). CD spectra characteristic of triple helices exhibit a positive molar ellipticity at 222−227 nm and a negative molar ellipticity at 195−200 nm (*61*). The CD spectra for (Gly-Pro-Hyp)$_4$-[IV-H1]-(Gly-Pro-Hyp)$_4$-NH_2, (Gly-Pro-Hyp)$_3$-Gly-Pro-[*cis*-Flp]-[IV-H1]-(Gly-Pro-Hyp)$_4$-NH_2, and (Gly-Pro-Hyp)$_3$-Gly-Pro-[*trans*-Flp]-[IV-H1]-(Gly-Pro-Hyp)$_4$-NH_2 are indicative of triple-helical

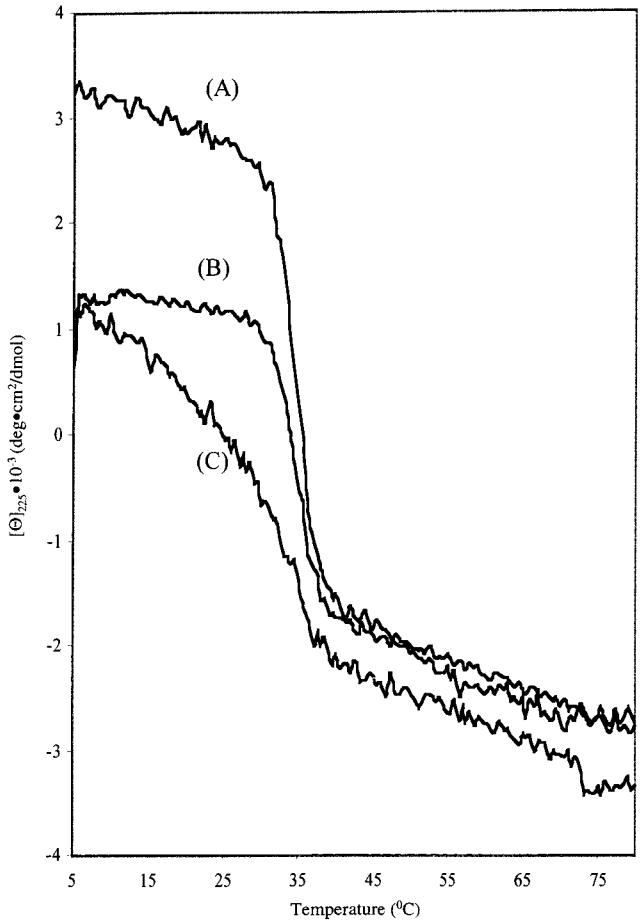

FIGURE 3: Temperature dependence of molar ellipticity at 225 nm for (A) (Gly-Pro-Hyp)$_3$-Gly-Pro-[*trans*-Flp]-[IV-H1]-(Gly-Pro-Hyp)$_4$-NH_2, (B) (Gly-Pro-Hyp)$_4$-[IV-H1]-(Gly-Pro-Hyp)$_4$-NH_2, and (C) (Gly-Pro-Hyp)$_3$-Gly-Pro-[*cis*-Flp]-[IV-H1]-(Gly-Pro-Hyp)$_4$-NH_2. Peptide concentrations were 3.41 μM in H_2O.

structure. (Gly-Pro-Hyp)$_3$-Gly-Pro-[*trans*-Flp]-[IV-H1]-(Gly-Pro-Hyp)$_4$-NH_2 exhibited the highest positive molar ellipticity, at 222.7 nm. (Gly-Pro-Hyp)$_4$-[IV-H1]-(Gly-Pro-Hyp)$_4$-NH_2 had a slightly lower positive molar ellipticity, at 221 nm. (Gly-Pro-Hyp)$_3$-Gly-Pro-[*cis*-Flp]-[IV-H1]-(Gly-Pro-Hyp)$_4$-NH_2 has the smallest positive molar ellipticity, at 224.2 nm.

To examine the thermal stability of the three peptides, the molar ellipticity at 225 nm was monitored as a function of increasing temperature. A triple-helical assembly can be distinguished from a simple, nonintercoiled poly-Pro II structure by its thermal denaturation behavior. A triple helix is relatively sensitive to temperature, and thus, triple-helical melts are highly cooperative (*61*). Both (Gly-Pro-Hyp)$_4$-[IV-H1]-(Gly-Pro-Hyp)$_4$-NH_2 and (Gly-Pro-Hyp)$_3$-Gly-Pro-[*trans*-Flp]-[IV-H1]-(Gly-Pro-Hyp)$_4$-NH_2 exhibited sigmoidal transitions, consistent with the melting of a triple helix to a single-stranded structure (Figure 3). The T_m values for (Gly-Pro-Hyp)$_4$-[IV-H1]-(Gly-Pro-Hyp)$_4$-NH_2 and (Gly-Pro-Hyp)$_3$-Gly-Pro-[*trans*-Flp]-[IV-H1]-(Gly-Pro-Hyp)$_4$-NH_2 were 34 and 37 °C, respectively (Table 2). The molar ellipticity of (Gly-Pro-Hyp)$_3$-Gly-Pro-[*cis*-Flp]-[IV-H1]-(Gly-Pro-Hyp)$_4$-NH_2 decreased very gradually between 5 and 30 °C and then markedly between 30 and 40 °C, followed by a gradual decrease until 80 °C (Figure 3). This broad melting curve is typical of "destabilized" triple helices, such as those containing D-amino acids or interruptions in the Gly-Xxx-Yyy repeating sequence (*62*−*64*), but is distinct from the near-linear decrease in molar ellipticity as a function of temperature observed for non-triple-helical species (*38*, *62*, *64*). The approximate T_m for (Gly-Pro-Hyp)$_3$-Gly-Pro-[*cis*-Flp]-[IV-H1]-(Gly-Pro-Hyp)$_4$-NH_2 was 30 °C (Table 2).

The ^{1}H NMR spectra for (Gly-Pro-Hyp)$_4$-[IV-H1]-(Gly-Pro-Hyp)$_4$-NH_2, (Gly-Pro-Hyp)$_3$-Gly-Pro-[*trans*-Flp]-[IV-H1]-(Gly-Pro-Hyp)$_4$-NH_2, and (Gly-Pro-Hyp)$_3$-Gly-Pro-[*cis*-Flp]-[IV-H1]-(Gly-Pro-Hyp)$_4$-NH_2 were recorded at 5 °C. For comparison to a non-triple-helical species, the spectrum of [IV-H1]-(Gly-Pro-Hyp)$_4$-NH_2 was used (*38*). The ^{1}H NMR spectra for the three triple-helical peptides were similar to each other (data not shown). One-dimensional ^{1}H NMR spectroscopy has been previously demonstrated to be an effective probe of triple-helical content (*38*, *65*−*67*). The ^{19}F NMR spectra were then recorded for (Gly-Pro-Hyp)$_3$-Gly-Pro-[*trans*-Flp]-[IV-H1]-(Gly-Pro-Hyp)$_4$-NH_2 and (Gly-Pro-Hyp)$_3$-Gly-Pro-[*cis*-Flp]-[IV-H1]-(Gly-Pro-Hyp)$_4$-NH_2. The ^{19}F NMR spectrum of (Gly-Pro-Hyp)$_3$-Gly-Pro-[*cis*-Flp]-[IV-H1]-(Gly-Pro-Hyp)$_4$-NH_2 at 5 °C exhibited a single major peak at −174.6 ppm. This result is similar to the single major peak observed for Boc-*cis*-Flp at −175.9 ppm (*53*). The ^{19}F NMR spectrum of (Gly-Pro-Hyp)$_3$-Gly-Pro-[*trans*-Flp]-[IV-H1]-(Gly-Pro-Hyp)$_4$-NH_2 at 5 °C exhibited three major peaks at −177.54, −177.56, and −177.58 ppm. This result is substantially different from the single major peak observed for Boc-*trans*-Flp at −178.5 ppm (*53*). Clearly, the effects of the triple-helical environment are different for *cis*-Flp and *trans*-Flp. The nature of these effects on the ^{19}F NMR spectra will be further explored elsewhere.

To assess the biological effects of Flp, we prepared the peptide−amphiphile models of (Gly-Pro-Hyp)$_4$-[IV-H1]-(Gly-Pro-Hyp)$_4$-NH_2, (Gly-Pro-Hyp)$_3$-Gly-Pro-[*trans*-Flp]-[IV-H1]-(Gly-Pro-Hyp)$_4$-NH_2, and (Gly-Pro-Hyp)$_3$-Gly-Pro-[*cis*-Flp]-[IV-H1]-(Gly-Pro-Hyp)$_4$-NH_2. Prior work has shown that construction of peptide−amphiphile species, whereby an alkyl chain is incorporated onto the N-terminus of a peptide, results in enhanced thermal stability of the peptide conformation and improved binding to hydrophobic surfaces (*10*, *34*, *37*, *38*, *68*). Biophysical studies were repeated for all three peptide−amphiphile constructs. The melting temperatures were 42.0, 47.0, and 35.5 °C for C_{16}-(Gly-Pro-Hyp)$_4$-[IV-H1]-(Gly-Pro-Hyp)$_4$-NH_2, C_{16}-(Gly-Pro-Hyp)$_3$-Gly-Pro-[*trans*-Flp]-[IV-H1]-(Gly-Pro-Hyp)$_4$-NH_2, and C_{16}-(Gly-Pro-Hyp)$_3$-Gly-Pro-[*cis*-Flp]-[IV-H1]-(Gly-Pro-Hyp)$_4$-NH_2, respectively (Table 2). These T_m values are sufficient for analysis of cellular activities. The T_m of 42.0 °C for C_{16}-(Gly-Pro-Hyp)$_4$-[IV-H1]-(Gly-Pro-Hyp)$_4$-NH_2 is considerably lower than the T_m value reported previously for this peptide−amphiphile construct (*38*). However, the peptide−amphiphile concentration for the earlier study was 0.5 mM (*38*), which causes more extensive aggregation and a correspondingly higher T_m value (*68*). The peptide−amphiphile concentration used for the CD analysis described herein (3.41 μM) approximates the concentration range required for biological studies (see below).

Melanoma Cell Adhesion and Spreading. Human melanoma cell adhesion was examined for C_{16}-(Gly-Pro-Hyp)$_4$-[IV-H1]-(Gly-Pro-Hyp)$_4$-NH_2, C_{16}-(Gly-Pro-Hyp)$_3$-Gly-Pro-[*trans*-Flp]-[IV-H1]-(Gly-Pro-Hyp)$_4$-NH_2, and C_{16}-(Gly-Pro-Hyp)$_3$-Gly-Pro-[*cis*-Flp]-[IV-H1]-(Gly-Pro-Hyp)$_4$-NH_2. The

Table 2: T_m Values for Triple Helix ⇔ Coil Transitions

peptide or peptide−amphiphile[a]	T_m (°C)
(Gly-Pro-Hyp)$_4$-[IV-H1]-(Gly-Pro-Hyp)$_4$-NH_2	34.0
(Gly-Pro-Hyp)$_3$-Gly-Pro-[*trans*-Flp]-[IV-H1]-(Gly-Pro-Hyp)$_4$-NH_2	37.0
(Gly-Pro-Hyp)$_3$-Gly-Pro-[*cis*-Flp]-[IV-H1]-(Gly-Pro-Hyp)$_4$-NH_2	30.0
C_{16}-(Gly-Pro-Hyp)$_4$-[IV-H1]-(Gly-Pro-Hyp)$_4$-NH_2	42.0
C_{16}-(Gly-Pro-Hyp)$_3$-Gly-Pro-[*trans*-Flp]-[IV-H1]-(Gly-Pro-Hyp)$_4$-NH_2	47.0
C_{16}-(Gly-Pro-Hyp)$_3$-Gly-Pro-[*cis*-Flp]-[IV-H1]-(Gly-Pro-Hyp)$_4$-NH_2	35.5

[a] [IV-H1] is Gly-Val-Lys-Gly-Asp-Lys-Gly-Asn-Pro-Gly-Trp-Pro-Gly-Ala-Pro.

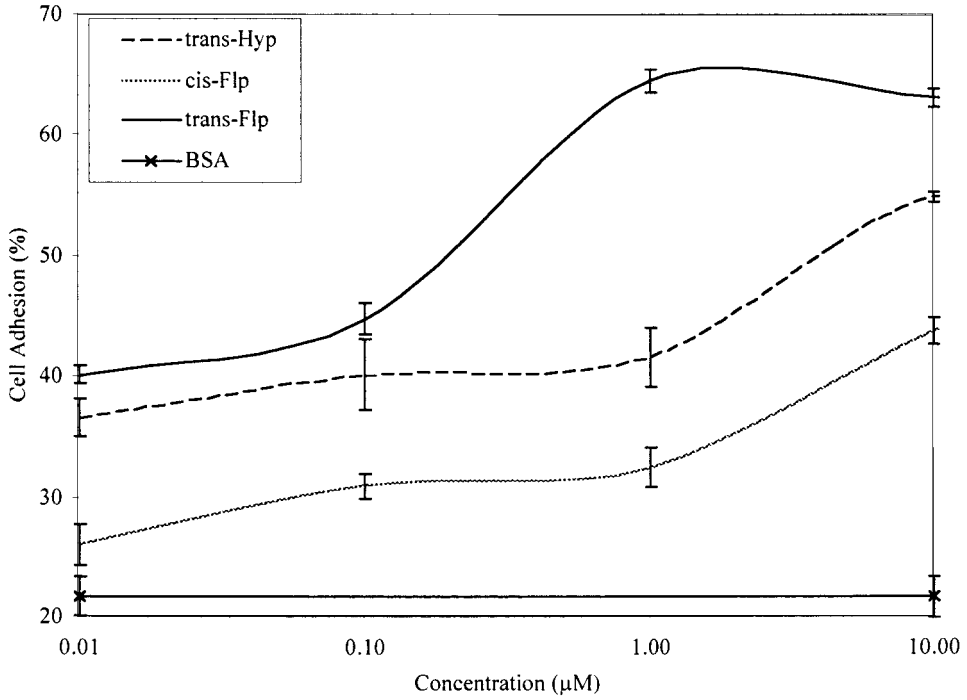

FIGURE 4: Human melanoma cell adhesion to C_{16}-(Gly-Pro-Hyp)$_4$-[IV-H1]-(Gly-Pro-Hyp)$_4$-NH_2 (—), C_{16}-(Gly-Pro-Hyp)$_3$-Gly-Pro-[*trans*-Flp]-[IV-H1]-(Gly-Pro-Hyp)$_4$-NH_2 (− − −), C_{16}-(Gly-Pro-Hyp)$_3$-Gly-Pro-[*cis*-Flp]-[IV-H1]-(Gly-Pro-Hyp)$_4$-NH_2 (···), type IV collagen (×), or BSA.

trans-Flp peptide−amphiphile construct promoted significant adhesion of melanoma cells, with an EC_{50} value of ∼0.35 μM (Figure 4). This compares to an EC_{50} value of ∼2.5 μM for C_{16}-(Gly-Pro-Hyp)$_4$-[IV-H1]-(Gly-Pro-Hyp)$_4$-NH_2 (Figure 4). The *cis*-Flp peptide−amphiphile construct promoted decreased levels of adhesion of melanoma cells, with an EC_{50} value of >5.0 μM (Figure 4). Over the concentration range that was studied, C_{16}-(Gly-Pro-Hyp)$_3$-Gly-Pro-[*trans*-Flp]-[IV-H1]-(Gly-Pro-Hyp)$_4$-NH_2 promoted the highest levels of cell adhesion, followed by C_{16}-(Gly-Pro-Hyp)$_4$-[IV-H1]-(Gly-Pro-Hyp)$_4$-NH_2, while adhesion to C_{16}-(Gly-Pro-Hyp)$_3$-Gly-Pro-[*cis*-Flp]-[IV-H1]-(Gly-Pro-Hyp)$_4$-NH_2 did not reach a maximum (Figure 4). Neither the [IV-H1] (linear) peptide nor the C_{16} tail alone produced significant adhesion over this range (*34*). To examine whether adhesion levels were due to variations in ligand packing density, adhesion experiments were repeated using 1:1 molar mixtures of the peptide−amphiphile construct and C_{16} tail (palmitic acid). Previous work had shown that the surface distribution of the peptide−amphiphile construct can influence cellular activities (*10*, *34*, *69*). Melanoma cell adhesion was improved for the peptide−amphiphile/palmitic acid mixtures compared to the peptide−amphiphile construct alone (data not shown), but the relative differences between each peptide−amphiphile construct for promotion of cell adhesion remained the same.

The ability of C_{16}-(Gly-Pro-Hyp)$_4$-[IV-H1]-(Gly-Pro-Hyp)$_4$-NH_2, C_{16}-(Gly-Pro-Hyp)$_3$-Gly-Pro-[*trans*-Flp]-[IV-H1]-(Gly-Pro-Hyp)$_4$-NH_2, and C_{16}-(Gly-Pro-Hyp)$_3$-Gly-Pro-[*cis*-Flp]-[IV-H1]-(Gly-Pro-Hyp)$_4$-NH_2 to promote cell spreading was next studied. Spreading was quantitated over a ligand concentration range of 0.01−50 μM (Figure 5). In a fashion similar to adhesion, melanoma cell spreading was more extensive on C_{16}-(Gly-Pro-Hyp)$_3$-Gly-Pro-[*trans*-Flp]-[IV-H1]-(Gly-Pro-Hyp)$_4$-NH_2 than on C_{16}-(Gly-Pro-Hyp)$_4$-[IV-H1]-(Gly-Pro-Hyp)$_4$-NH_2 at higher ligand concentrations (1−50 μM). Very low levels of spreading were observed with C_{16}-(Gly-Pro-Hyp)$_3$-Gly-Pro-[*cis*-Flp]-[IV-H1]-(Gly-Pro-Hyp)$_4$-NH_2 at all concentrations that were tested. Representative microscopic images of melanoma cell spreading on 10 μM C_{16}-(Gly-Pro-Hyp)$_3$-Gly-Pro-[*trans*-Hyp]-[IV-H1]-(Gly-Pro-Hyp)$_4$-NH_2, 1 μM C_{16}-(Gly-Pro-Hyp)$_3$-Gly-Pro-[*trans*-Flp]-[IV-H1]-(Gly-Pro-Hyp)$_4$-NH_2, and 50 μM C_{16}-(Gly-Pro-Hyp)$_3$-Gly-Pro-[*cis*-Flp]-[IV-H1]-(Gly-Pro-Hyp)$_4$-NH_2 (Figure 6) illustrate the variation in cell activity based on ligand.

DISCUSSION

The development of model triple-helical peptide ligands (*7*−*13*, *15*) has led to a better understanding of the role of the triple helix as a modulator of biological function. As these

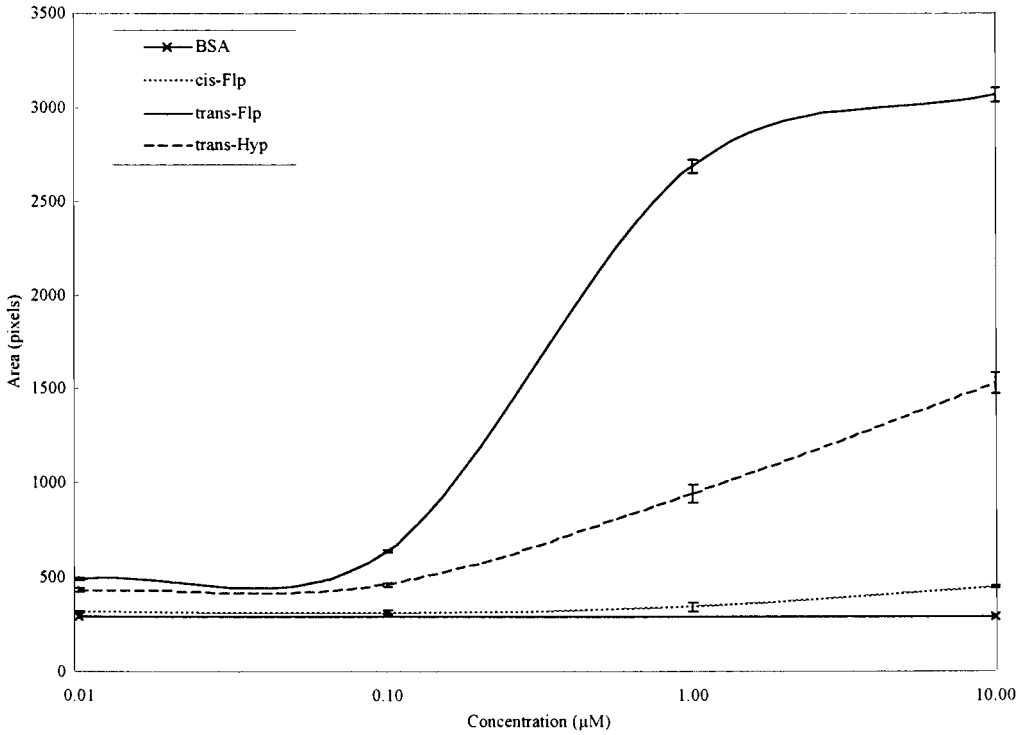

FIGURE 5: Human melanoma cell spreading on C_{16}-(Gly-Pro-Hyp)$_4$-[IV-H1]-(Gly-Pro-Hyp)$_4$-NH_2 (—), C_{16}-(Gly-Pro-Hyp)$_3$-Gly-Pro-[*trans*-Flp]-[IV-H1]-(Gly-Pro-Hyp)$_4$-NH_2 (– – –), C_{16}-(Gly-Pro-Hyp)$_3$-Gly-Pro-[*cis*-Flp]-[IV-H1]-(Gly-Pro-Hyp)$_4$-NH_2 (···), type IV collagen (thin solid line), or BSA (thick solid line) at 37 °C. Peptide−amphiphile concentrations were 0.01−50 μM.

triple-helical models have become more sophisticated, subtle questions related to triple-helical modulation of cellular activities may be asked. We have previously examined melanoma cell interaction with the α1(IV)1263−1277 ([IV-H1]) sequence in one of four conformational contexts: monomeric single-stranded, clustered single-stranded, monomeric triple-helical, and clustered triple-helical ligand (*34*). Dramatic differences were observed in cell adhesion and signal transduction for single-stranded versus triple-helical sequences (*34*). Melanoma cell interaction with the [IV-H1] region was clearly conformationally dependent. To further dissect the mechanisms of melanoma cell behavior, it is necessary to develop ligands that have differences in their relative triple-helical content, rather than simply being triple-helical versus non-triple-helical. Substitution of (Gly-Pro-Hyp)$_4$-[IV-H1]-(Gly-Pro-Hyp)$_4$-NH_2 with either *trans*-Flp or *cis*-Flp could create ligands that have either enhanced or reduced triple helicity compared to the parent ligand.

To incorporate *trans*-Flp and *cis*-Flp into the desired ligands, more convenient methods were developed for the synthesis of Flp derivatives. The primary improvement was the use of the benzyl group to protect the carboxyl terminus of Hyp. *trans*-Hyp-OBzl is commercially available, and the benzyl group is easily removed by CTH. Peptides and peptide−amphiphile constructs were assembled with the Yyy_{12} position of (Gly-Pro-Hyp)$_3$-Gly-Pro-Yyy-[IV-H1]-(Gly-Pro-Hyp)$_4$-NH_2 containing *trans*-Hyp, *cis*-Flp, or *trans*-Flp. Overall, the CD spectroscopic studies have shown that substitution of a single *trans*-Flp residue with a *trans*-Hyp residue slightly increased the thermal stability of the model peptide, while substitution of a single *cis*-Flp residue substantially decreased the thermal stability. These results are consistent with prior studies of Flp residue effects on triple-helix stability (*4*, *5*, *23*). Substitution of all of the *trans*-Hyp residues in (Pro-Hyp-Gly)$_{10}$ or (Pro-Hyp-Gly)$_7$ with *trans*-Flp increased the T_m values by 22 and 9 °C, respectively (*4*, *5*, *23*). Conversely, an analogous substitution in (Pro-Hyp-Gly)$_7$ with *cis*-Flp dramatically decreased T_m by greater than 26 °C (*23*). The relative effects of *trans*-Hyp, *trans*-Flp, and *cis*-Flp coincide with their propensity for forming *trans*-peptide bonds compared to *cis*-peptide bonds (*70*, *71*). This "inductive effect," based on the electronegativity and stereochemistry of the 4-substituent in the pyrrolidine ring system, is an important contributor to triple-helix stability (*4*, *5*, *47*, *70*), but had only been examined previously in the context of identical repeating triplets [i.e., (Pro-Hyp-Gly)$_{10}$, (Pro-*trans*-Flp-Gly)$_{10}$, (Pro-*trans*-Flp-Gly)$_7$, (Pro-*cis*-Flp-Gly)$_7$, etc.]. Our study demonstrates that even a single substitution of *trans*-Hyp with *trans*-Flp or *cis*-Flp can have a significant impact on triple-helix stability. Thus, modulation of triple-helical structural stability, which could prove to be important in the design of triple-helical ligands and substrates and be the basis for development of new collagen model biomaterials, can be achieved by judicious incorporation of Hyp and Flp residues. Also, the combination of Flp incorporation and ^{19}F NMR spectroscopy may provide for an additional probe of triple-helical environment.

Melanoma cell adhesion to the three ligands suggested dramatic biological consequences of even subtle changes in relative triple-helical content. The most stable triple helix promoted adhesion the most efficiently. A relatively small decrease in triple-helical stability (~5 °C) corresponded to a significant decrease in the level of adhesion promotion. A further decrease in triple-helical stability (~6.5 °C) resulted in a proportionally smaller amount of adhesion. Promotion of melanoma cell spreading had trends similar, but not identical, to those seen for cell adhesion. Again, a relatively small decrease in triple-helical stability (~5 °C) substantially

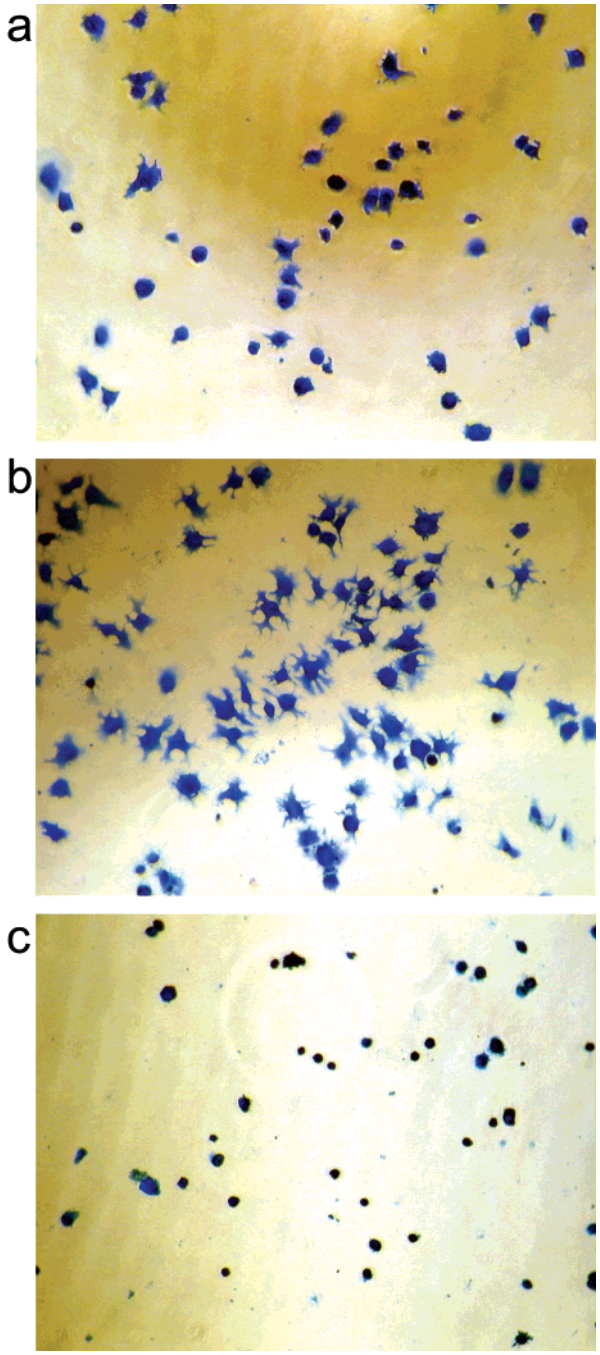

FIGURE 6: Human melanoma cell spreading on (a) 10 μM C_{16}-(Gly-Pro-Hyp)$_4$-[IV-H1]-(Gly-Pro-Hyp)$_4$-NH_2, (b) 1 μM C_{16}-(Gly-Pro-Hyp)$_3$-Gly-Pro-[*trans*-Flp]-[IV-H1]-(Gly-Pro-Hyp)$_4$-NH_2, or (c) 50 μM C_{16}-(Gly-Pro-Hyp)$_3$-Gly-Pro-[*cis*-Flp]-[IV-H1]-(Gly-Pro-Hyp)$_4$-NH_2 at 37 °C.

decreased the level of cell spreading. A further decrease in triple-helical stability (~6.5 °C) resulted in almost negligible spreading. The adhesion and spreading effects do not appear to be the result of the Flp residues per se, as (a) the Flp residue is located outside of the active site region of [IV-H1] and (b) cellular responses are different for *trans*-Flp and *cis*-Flp ligands, and it is doubtful that cell receptors are exquisitely sensitive to the orientation of the fluorine atom alone. Prior studies have indicated that melanoma cell recognition of [IV-H1] is based on electrostatic interactions (*72*). Thus, it is unlikely that a relatively minor change in primary structure (*cis*-Flp to *trans*-Flp) unrelated to ligand charge will play a larger role in modulating cell adhesion and spreading.

The cell studies performed herein have utilized partially denatured ligands. Are these ligands in an equilibrium between triple-helical and unfolded molecules, or are they an intermediate, partially folded structure? The cell adhesion and spreading data suggest the latter scenario. For example, one can compare the levels of adhesion or spreading with the relative "concentration" of triple-helical species. At 37 °C, the *trans*-Flp peptide−amphiphile construct is <10% denatured while the *cis*-Flp peptide−amphiphile construct is ~65% denatured (Table 2). If an equilibrium between triple-helical and unfolded molecules existed, than a 10 μM solution of the *cis*-Flp peptide−amphiphile construct would contain 3.5 μM triple-helical species and 6.5 μM unfolded species. However, at a concentration of 3.5 μM, the *cis*-Flp peptide−amphiphile construct still does not promote cell adhesion or spreading at levels comparable to the *trans*-Flp peptide−amphiphile construct (Figure 5). Further analysis of the cell spreading data also suggests the existence of an intermediate, partially folded species. If only an equilibrium existed, then we would expect to see some cells (those bound to the triple-helical species) spread equally well on C_{16}-(Gly-Pro-Hyp)$_3$-Gly-Pro-[*cis*-Flp]-[IV-H1]-(Gly-Pro-Hyp)$_4$-NH_2 as cells interacting with the C_{16}-(Gly-Pro-Hyp)$_3$-Gly-Pro-[*trans*-Flp]-[IV-H1]-(Gly-Pro-Hyp)$_4$-NH_2 peptide−amphiphile construct. However, such results are not observed (Figure 6). Instead, we observe a consistently lower level of spreading induced by C_{16}-(Gly-Pro-Hyp)$_3$-Gly-Pro-[*cis*-Flp]-[IV-H1]-(Gly-Pro-Hyp)$_4$-NH_2 than by C_{16}-(Gly-Pro-Hyp)$_3$-Gly-Pro-[*trans*-Flp]-[IV-H1]-(Gly-Pro-Hyp)$_4$-NH_2, implying that the cells are interacting with a folding intermediate.

Melanoma cell interaction with the [IV-H1] ligands is via CD44−chondrotin sulfate proteoglycan (*31*). Clearly, CD44 interaction with this site, and subsequent promotion of signaling and spreading activities, is dependent upon the triple-helical conformation. However, the role of CD44 in tumor cell invasion has not been well defined. CD44 and several isoforms have been characterized on a variety of tumor cell surfaces (*73*−*75*), and have been suggested to be prognostic indicators of malignant melanoma (*76*). Although CD44 binds to collagen types I, IV, VI, and XIV, it is not a primary receptor for cell adhesion to collagen (*36*, *77*−*79*). CD44 has been shown to play a role in two-dimensional melanoma cell migration on collagen types I and IV (*36*, *79*), but melanoma cell motility on three-dimensional collagen lattices does not involve CD44 and results in shedding of this receptor (*80*, *81*). Finally, the CD44 cytoplasmic domain binds to ankyrin and members of the ezrin−radixin−moesin (ERM) family of cytoskeletal proteins (*75*). Binding to ankyrin may be the first step in intracellular signaling by CD44, which then leads to Src kinase activity (*75*). One result of CD44 outside-in signaling is upregulation and activation of integrins (*82*).

We have previously described a "collagen structural modulation" mechanism that may exist for tumor cell invasion, whereby triple-helical collagen promotes cell binding and induction of signal transduction, subsequently leading to collagen dissolution by proteases, decreased binding and signal transduction levels, and enhanced tumor cell motility (*12*). This mechanism was based on studies of melanoma cell interaction with the $\alpha 3\beta 1$ integrin specific

ligand α1(IV)531−543, in both triple-helical and non-triple-helical conformations (*8*, *12*, *83*, *84*). Results from the present and prior (*7*, *10*, *34*) studies with the CD44 specific ligand α1(IV)1263−1277 ([IV-H1]) are also consistent with the collagen structural modulation mechanism. The interaction of CD44 with the α1(IV)1263−1277 region is most likely a postadhesion event during invasion. Signaling and spreading are promoted by the native triple-helical structure. As the basement membrane is compromised by proteases, triple-helical structure is disrupted. Activities promoted by CD44 would then decrease. The disruption of the triple helix would then result in (a) decreased affinity of the α1β1 and α2β1 integrin binding and (b) exposure of "cryptic" sites (*85*, *86*) which could aid in subsequent steps of invasion. Future studies will examine CD44 signaling as a function of relative ligand conformation and composition.

ACKNOWLEDGMENT

We thank Dr. W. Craig Byrdwell for the ESMS analyses and Dr. Frank Mari for assistance with the NMR experiments.

REFERENCES

1. Brodsky, B., and Shah, N. K. (1995) *FASEB J. 9*, 1537−1546.
2. Fields, G. B., and Prockop, D. J. (1996) *Biopolymers 40*, 345−357.
3. Brodsky, B., and Ramshaw, J. A. M. (1997) *Matrix Biol. 15*, 545−554.
4. Holmgren, S. K., Taylor, K. M., Bretscher, L. E., and Raines, R. T. (1998) *Nature 392*, 666−667.
5. Holmgren, S. K., Bretscher, L. E., Taylor, K. M., and Raines, R. T. (1999) *Chem. Biol. 6*, 63−70.
6. Persikov, A. V., Ramshaw, J. A. M., and Brodsky, B. (2000) *Biopolymers 55*, 436−450.
7. Fields, C. G., Mickelson, D. J., Drake, S. L., McCarthy, J. B., and Fields, G. B. (1993) *J. Biol. Chem. 268*, 14153−14160.
8. Miles, A. J., Skubitz, A. P. N., Furcht, L. T., and Fields, G. B. (1994) *J. Biol. Chem. 269*, 30939−30945.
9. Grab, B., Miles, A. J., Furcht, L. T., and Fields, G. B. (1996) *J. Biol. Chem. 271*, 12234−12240.
10. Yu, Y.-C., Pakalns, T., Dori, Y., McCarthy, J. B., Tirrell, M., and Fields, G. B. (1997) *Methods Enzymol. 289*, 571−587.
11. Morton, L. F., Peachey, A. R., Knight, C. G., Farndale, R. W., and Barnes, M. J. (1997) *J. Biol. Chem. 272*, 11044−11048.
12. Lauer, J. L., Gendron, C. M., and Fields, G. B. (1998) *Biochemistry 37*, 5279−5287.
13. Knight, C. G., Morton, L. F., Peachey, A. R., Tuckwell, D. S., Farndale, R. W., and Barnes, M. J. (2000) *J. Biol. Chem. 275*, 35−40.
14. Emsley, J., Knight, C. G., Farndale, R. W., Barnes, M. J., and Liddington, R. C. (2000) *Cell 101*, 47−56.
15. Xu, Y., Gurusiddappa, S., Rich, R. L., Owens, R. T., Keene, D. R., Mayne, R., Höök, A., and Höök, M. (2000) *J. Biol. Chem. 275*, 38981−38989.
16. Morton, L. F., McCulloch, I. Y., and Barnes, M. J. (1993) *Thromb. Res. 72*, 367−372.
17. Morton, L. F., Hargreaves, P. G., Farndale, R. W., Young, R. D., and Barnes, M. J. (1995) *Biochem. J. 306*, 337−344.
18. Ackerman, M. S., Bhate, M., Shenoy, N., Beck, K., Ramshaw, J. A. M., and Brodsky, B. (1999) *J. Biol. Chem. 274*, 7668−7673.
19. Persikov, A. V., Ramshaw, J. A. M., Kirkpatrick, A., and Brodsky, B. (2000) *Biochemistry 39*, 14960−14967.
20. Babu, I. R., and Gamesh, K. N. (2001) *J. Am. Chem. Soc. 123*, 2079−2080.
21. Bann, J. G., Peyton, D. H., and Bächinger, H. P. (2000) *FEBS Lett. 473*, 237−240.
22. Bann, J. G., and Bächinger, H. P. (2000) *J. Biol. Chem. 275*, 24466−24469.
23. Bretscher, L. E., Taylor, K. M., and Raines, R. T. (2000) in *Peptides for the New Millennium* (Fields, G. B., Tam, J. P., and Barany, G., Eds.) pp 355−356, Kluwer Academic Publishers, Dordrecht, The Netherlands.
24. Tang, Y., Ghirlanda, G., Petka, W. A., Nakajima, T., DeGrado, W. F., and Tirrell, D. A. (2001) *Angew. Chem., Int. Ed. 40*, 1494−1496.
25. Tang, Y., Ghirlanda, G., Vaidehi, N., Kua, J., Mainz, D. T., Goddard, W. A., III, DeGrado, W. F., and Tirrell, D. A. (2001) *Biochemistry 40*, 2790−2796.
26. Bilgicer, B., Fichera, A., and Kumar, K. (2001) *J. Am. Chem. Soc. 123*, 4393−4399.
27. Mooney, E. F. (1970) *An Introduction to ^{19}F NMR Spectroscopy*, Hyden & Son Ltd.
28. Tonelli, A. E. (1989) *NMR Spectroscopy and Polymer Microstructure: The Conformational Connection*, VCH Publishers, New York.
29. Friebolin, H. (1998) *Basic One- and Two-Dimensional NMR Spectroscopy, Third Revised Edition*, VCH Publishers, New York.
30. Costa, J. L., Joy, D. C., Maher, D. M., Kirk, K. L., and Hui, S. W. (1978) *Science 200*, 537.
31. McCarthy, J. B., Vachhani, B., and Iida, J. (1996) *Biopolymers 40*, 371−381.
32. Chelberg, M. K., McCarthy, J. B., Skubitz, A. P. N., Furcht, L. T., and Tsilibary, E. C. (1990) *J. Cell Biol. 111*, 261−270.
33. Mayo, K. H., Parra-Diaz, D., McCarthy, J. B., and Chelberg, M. (1991) *Biochemistry 30*, 8251−8267.
34. Fields, G. B., Lauer, J. L., Dori, Y., Forns, P., Yu, Y.-C., and Tirrell, M. (1998) *Biopolymers 47*, 143−151.
35. Mickelson, D. J., Faassen, A. E., and McCarthy, J. B. (1991) *J. Cell Biol. 115*, 287a.
36. Knutson, J. R., Iida, J., Fields, G. B., and McCarthy, J. B. (1996) *Mol. Biol. Cell 7*, 383−396.
37. Yu, Y.-C., Berndt, P., Tirrell, M., and Fields, G. B. (1996) *J. Am. Chem. Soc. 118*, 12515−12520.
38. Yu, Y.-C., Tirrell, M., and Fields, G. B. (1998) *J. Am. Chem. Soc. 120*, 9979−9987.
39. Yu, Y.-C., Roontga, V., Daragan, V. A., Mayo, K. H., Tirrell, M., and Fields, G. B. (1999) *Biochemistry 38*, 1659−1668.
40. Middleton, W. J. (1975) *J. Org. Chem. 40*, 574−578.
41. Fields, G. B., Tian, Z., and Barany, G. (1992) in *Synthetic Peptides: A User's Guide* (Grant, G. A., Ed.) pp 77−183, W. H. Freeman & Co., New York.
42. Fields, C. G., VanDrisse, V. L., and Fields, G. B. (1993) *Pept. Res. 6*, 39−47.
43. Fields, C. G., and Fields, G. B. (1993) *Tetrahedron Lett. 34*, 6661−6664.
44. Henkel, W., Vogl, T., Echner, H., Voelter, W., Urbanke, C., Schleuder, D., and Rauterberg, J. (1999) *Biochemistry 38*, 13610−13622.
45. Hudlicky, M., and Merola, J. (1990) *Tetrahedron Lett. 31*, 7403−7406.
46. Hudlicky, M. (1993) *J. Fluorine Chem. 60*, 193−210.
47. Panasik, N., Jr., Eberhardt, E. S., Edison, A. S., Powell, D. R., and Raines, R. T. (1994) *Int. J. Pept. Protein Res. 44*, 262−269.
48. Kronenthal, D. R., Mueller, R. H., Kuester, P. L., Kissick, T. P., and Johnson, E. J. (1990) *Tetrahedron Lett. 31*, 1241−1244.
49. Gottlieb, A., Fujita, Y., Undenfriend, S., and Witkop, B. (1965) *Biochemistry 4*, 2507−2513.
50. Shirota, F. N., Nagasawa, H. T., and Elberling, J. A. (1977) *J. Med. Chem. 20*, 1176−1181.
51. Hart, B. P., and Coward, J. K. (1993) *Tetrahedron Lett. 34*, 4917−4920.
52. Avent, A. G., Bowler, A. N., Doyle, P. M., Marchand, C. M., and Young, D. W. (1992) *Tetrahedron Lett. 33*, 1509−1512.
53. Demange, L., Ménez, A., and Dugave, C. (1998) *Tetrahedron Lett. 39*, 1169−1172.
54. Tran, T. T., Patino, N., Condom, R., Frogier, T., and Guedj, R. (1997) *J. Fluorine Chem. 82*, 125−130.

55. Lloyd-Williams, P., Merzouk, A., Guibé, F., Albericio, F., and Giralt, E. (1994) *Tetrahedron Lett. 35*, 4437−4440.
56. Martinez, J., Tolle, J. C., and Bodanszky, M. (1979) *J. Org. Chem. 44*, 3596−3598.
57. Atherton, E., Bury, C., Sheppard, R. C., and Williams, B. J. (1979) *Tetrahedron Lett.*, 3041−3042.
58. Anwer, M. K., and Spatola, A. F. (1980) *Synthesis*, 929−932.
59. Anwer, M. K., Spatola, A. F., Bossinger, C. D., Flanigan, E., Liu, R. C., Olsen, D. B., and Stevenson, D. (1983) *J. Org. Chem. 48*, 3503−3507.
60. Kolbe, H. V. J., Lu, R. C., and Wohlrab, H. (1985) *J. Chromatogr. 327*, 1−7.
61. Heidemann, E., and Roth, W. (1982) *Adv. Polym. Sci. 43*, 143−203.
62. Long, C. G., Braswell, E., Zhu, D., Apigo, J., Baum, J., and Brodsky, B. (1993) *Biochemistry 32*, 11688−11695.
63. Shah, N. K., Brodsky, B., Kirkpatrick, A., and Ramshaw, J. A. M. (1999) *Biopolymers 49*, 297−302.
64. Beck, K., Chan, V. C., Shenoy, N., Kirkpatrick, A., Ramshaw, J. A. M., and Brodsky, B. (2000) *Proc. Natl. Acad. Sci. U.S.A. 97*, 4273−4278.
65. Long, C. G., Li, M. H., Baum, J., and Brodsky, B. (1992) *J. Mol. Biol. 225*, 1−4.
66. Brodsky, B., Li, N. H., Long, C. G., Apigo, J., and Baum, J. (1992) *Biopolymers 32*, 447−451.
67. Bhatnagar, R. S., Pattabiramam, N., Sorensen, K. R., Langridge, R., and MacElroy, R. D. (1988) *J. Biomol. Struct. Dyn. 6*, 223−233.
68. Forns, P., Lauer-Fields, J. L., Gao, S., and Fields, G. B. (2000) *Biopolymers 54*, 531−546.
69. Pakalns, T., Haverstick, K. L., Fields, G. B., McCarthy, J. B., Mooradian, D. L., and Tirrell, M. (1999) *Biomaterials 20*, 2265−2279.
70. Eberhardt, E. S., Panasik, J. N., and Raines, R. T. (1996) *J. Am. Chem. Soc. 118*, 12261−12266.
71. Bretscher, L. E., Jenkins, C. L., Taylor, K. M., DeRider, M. L., and Raines, R. T. (2001) *J. Am. Chem. Soc. 123*, 777−778.
72. McCarthy, J. B., Mickelson, D. J., Fields, C. G., and Fields, G. B. (1993) in *Peptides 1992* (Schneider, C. H., and Eberle, A. N., Eds.) pp 109−110, Escom Science Publishers, Leiden, The Netherlands.
73. Kincade, P. W., Zheng, Z., Katoh, S., and Hanson, L. (1997) *Curr. Opin. Cell Biol. 9*, 635−642.
74. Lesley, J., Hyman, R., English, N., Catterall, J. B., and Turner, G. A. (1997) *Glycoconjugate J. 14*, 611−622.
75. Bourguignon, L. Y. W., Zhu, D., and Zhu, H. (1998) *Front. Biosci. 3*, 637−649.
76. Leigh, C. J., Palechek, P. L., Knutson, J. R., McCarthy, J. B., Cohen, M. B., and Argenyi, Z. B. (1996) *Hum. Pathol. 27*, 1288−1294.
77. Carter, W. G., and Wayner, E. A. (1989) *J. Biol. Chem. 263*, 4193−4201.
78. Ehnis, T., Dieterich, W., Bauer, M., von Lampe, B., and Shuppan, D. (1996) *Exp. Cell Res. 229*, 388−397.
79. Faassen, A. E., Schrager, J. A., Klein, D. J., Oegema, T. R., Couchman, J. R., and McCarthy, J. B. (1992) *J. Cell Biol. 116*, 521−531.
80. Friedl, P., Maaser, K., Klein, C. E., Niggemann, B., Krohne, G., and Zanker, K. S. (1997) *Cancer Res. 57*, 2061−2070.
81. Maaser, K., Wolf, K., Klein, C. E., Niggemann, B., Zänker, K. S., Bröcker, E.-B., and Friedl, P. (1999) *Mol. Biol. Cell 10*, 3067−3079.
82. Fujisaki, T., Tanaka, Y., Fujii, K., Mine, S., Saito, K., Yamada, S., Yamashita, U., Irimura, T., and Eto, S. (1999) *Cancer Res. 59*, 4427−4434.
83. Miles, A. J., Knutson, J. R., Skubitz, A. P. N., Furcht, L. T., McCarthy, J. B., and Fields, G. B. (1995) *J. Biol. Chem. 270*, 29047−29050.
84. Li, C., McCarthy, J. B., Furcht, L. T., and Fields, G. B. (1997) *Biochemistry 36*, 15404−15410.
85. Xu, J., Rodriguez, D., Petitclerc, E., Kim, J. J., Hangai, M., Yuen, S. M., Davis, G. E., and Brooks, P. C. (2001) *J. Cell Biol. 154*, 1069−1080.
86. Fields, G. B. (1995) *Connect. Tissue Res. 31*, 235−243.

BI012071W